Mutations of the B-Cell Receptor Pathway Confer Chemoresistance in Primary Cutaneous Diffuse Large B-Cell Lymphoma Leg Type

Océane Ducharme, Marie Beylot-Barry, Anne Pham-Ledard, Elodie Bohers, Pierre-Julien Viailly, Thomas Bandres, Nicolas Faur, Éric Frison, Béatrice Vergier, Fabrice Jardin, et al.

Mutations of the B-cell receptor pathway confer chemoresistance in primary cutaneous diffuse large B-cell lymphoma leg-type

Océane Ducharme[1,2], Marie Beylot-Barry[1,2], Anne Pham-Ledard[1,2], Elodie Bohers[6], Pierre-Julien Viailly[6], Thomas Bandres[3], Nicolas Faur[3], Eric Frison[4], Béatrice Vergier[2,5], Fabrice Jardin[6], Jean-Philippe Merlio[2,3], Audrey Gros[2,3]

Authors' affiliations :

[1]Service de Dermatologie, CHU de Bordeaux, Bordeaux, France

[2]INSERM U1053, Equipe Oncogenèse des lymphomes cutanés, Université de Bordeaux

[3]Service de Biologie des tumeurs, CHU de Bordeaux, Pessac, France

[4] Service d'information médicale, CHU Bordeaux, Bordeaux, France.

[5]Service d'Anatomie pathologique, CHU de Bordeaux, Pessac, France

[6]INSERM U1245 and Centre Henri Becquerel 76038 Rouen, France

Corresponding Author:

Audrey Gros

1. Université de Bordeaux Collège Sciences de la Santé, INSERM U1053 Team Oncogenesis of Cutaneous Lymphomas
Bordeaux, Aquitaine, FR
+33557571027

2. CHU Bordeaux, Tumor Bank and Tumor Biology Laboratory
Bordeaux, Aquitaine, FR
+33557656011

audrey.gros@chu-bordeaux.fr

Tel : 05 57 65 60 11

Fax : 05 57 57 10 32

Text word count: 3500/3500

Abstract word count: 195/200

Figures and tables: 4 figures, 2 tables

Supplementary Material: 5 figures, 2 tables

Key words: Primary cutaneous diffuse large B-cell lymphoma, leg type; Next generation sequencing; B-cell receptor

Abbreviations used:

ABC: Activated B-cell like

AID: Activation-induced cytidine deaminase

ASHM: Aberrant somatic hypermutation

BCR: B-cell receptor

BTK: Bruton Tyrosine Kinase

CNV: Copy Number Variation

CR: Patients with durable complete response

DLBCL: Diffuse large B-cell lymphoma

FFPE: Formalin-Fixed, Paraffin-Embedded

GCB: Germinal center B-cell like

INDEL: Insertion – Deletion

NGS: Next Generation Sequencing

NF-κB: Nuclear factor-kappa B

OS: Overall survival

PCLBCL-LT: Primary cutaneous diffuse large B-cell lymphoma, leg type

PCNSL: Primary Central Nervous System Lymphoma

PFS: Progression-free survival

RR: Patients with relapsing or refractory disease

R-PCT: Rituximab and polychemotherapy

SNV: Single Nucleotide Variation

SS: Specific Survival

WES: Whole Exome Sequencing

ABSTRACT

Primary cutaneous diffuse large B-cell lymphoma leg-type (PCLBCL-LT) preferentially involves the lower limb in elderly subjects. A combination of poly-chemotherapy with Rituximab has improved prognosis. However, about 50% of patients will experience progression or relapse without any predictive biologic marker of therapeutic response. The mutational profile of PLCBCL-LT has highlighted mutations contributing to constitutive NF-κB and B-cell receptor (BCR) signaling pathways but has not demonstrated clinical utility. Therefore, the mutational status of 32 PCLBCL-LT, 14 patients with complete durable response and 18 with relapsing/refractory disease was determined with a dedicated lymphopanel. Tumors pairs at diagnosis and relapse or progression were analyzed in 14 relapsing/refractory patients.

PCLBCL-LT patients harboring one mutation that targets one of the following BCR signaling genes (*CD79A/B* or *CARD11*) displayed a reduced progression-free survival and specific survival (median 18 months, P=0.002 and 51 months, P=0.03 respectively, whereas median duration in wild type group was not reached) and were associated with therapeutic resistance (P=0.0006). Longitudinal analyses revealed that *MYD88* and *CD79B* were the earliest and among the most mutated genes. Our data suggest that evaluating BCR mutations in patients with PCLBCL-LT may help to predict first-line therapeutic response and to select targeted therapies.

INTRODUCTION:

Primary cutaneous diffuse large B-cell lymphoma leg-type (PCLBCL-LT) has been individualized as an aggressive disease accounting for 5% of primary cutaneous lymphoma and for 20% of primary cutaneous B-cell lymphoma (Willemze et al., 2019, 2005). Occurring especially in elderly women, it presents mostly as tumor and nodules, preferentially involving the lower limb (Grange et al., 2007; Willemze et al., 2005). PCLBCL-LT correspond to a monotonous infiltrate of confluent sheets of centroblasts and immunoblasts typically expressing CD20, CD79a, Bcl-2 and MUM-1/IRF4 with usual negativity for CD5 and CD10 (Menguy et al., 2016; Swerdlow et al., 2016; Willemze et al., 2005). Morphology and phenotype bring PCLBCL-LT close to the specific activated B-cell (ABC) subtype of diffuse large B-cell lymphoma (DLBCL) which has been individualized by gene expression profiling from "Germinal center B-cell like" (GCB) and primary mediastinal B-cell lymphoma (Alizadeh et al., 2000). Such ABC subtype corresponds to a post germinal center (GC) cell of origin with constitutive activation of nuclear factor-kappa B (NF-κB) signaling pathway and a poorer outcome. Molecular profiling of PCLBCL-LT further supported its relationship with the ABC DLBCL subtype (Hoefnagel, 2005; Pham-Ledard et al., 2013). A combination of poly-chemotherapy with a CD20-directed monoclonal antibody Rituximab (R-PCT), adapted to the age of patients has improved the prognosis (average 5-year survival: 73%) (Grange et al., 2014). After CD20 binding, rituximab exerts several antitumoral effects either by directly triggering antiproliferative effects through calcium release or influx, Src kinase activation and apoptosis through BCL2 down regulation or by indirectly mediating complement-dependent cytotoxicity (CDC) or antibody-dependent cell-mediated cytotoxicity/phagocytosis (ADCC/ADCP) through Fc-γ binding by immune cells (Bachy and Salles, 2014; Chao, 2013). About half of patients will experience cutaneous or extra cutaneous relapse and progression

with death due to disease without any biologic marker that could predict R-PCT response (Grange et al., 2014; Senff et al., 2008).

Moreover, PCLBCL-LT has peculiar genetic features with a dramatic prevalence of the *MYD88*^{L265P} mutation in around 70% of cases (Pham-Ledard et al., 2012, 2014). Mutations leading to the activation of the B-cell receptor pathway and to NF-κB activation were first detected by targeted analyses (Koens et al., 2014; Pham-Ledard et al., 2014). Using whole exome sequencing (WES) and a dedicated lymphopanel, a restricted set of highly recurrent mutations of *MYD88, PIM1, CD79B* and *MYC*, as well as *CDKN2A*, *PRDM1* and *TNFAIP3* deletions were found to associate in 32 patients (Mareschal et al., 2017). Indeed, PCLBCL-LT mutational profile is closer to that of primary central nervous system lymphoma (PCNSL) than to other DLBCL subtypes, a finding recently confirmed by another WES study of 19 cases of PCLBCL-LT (Mareschal et al., 2017; Zhou et al., 2018).

This present study aimed at evaluating if the mutational status of 36 genes involved in B-cell lymphomagenesis may help to differentiate among 32 patients with PCLBCL-LT those who experienced after R-PCT complete durable response (CR) or presented relapsing-refractory (RR) disease. Our second objective was to compare tumors pairs at diagnosis and at relapse or progression in 14 patients.

RESULTS:

Clinico-pathological features:

Our cohort comprised 32 patients, mostly women (59%), with a median age at diagnosis of 81 years (range, 61 to 97), preferentially involving the legs (27/32, 84%) **(Table 1)**. All PCLBCL-LT cases expressed BCL2, MUM1, CD20 and were negative for CD10. Most cases were positive for BCL6 (72%) **(Supplementary Table S1 online)**. Such profile indicated an ABC-subtype according to the modified Hans' algorithm (Menguy et al., 2019). After initial

therapy by R-PCT, 14 patients (44%) reached complete durable response (CR) with a median of 39 months (range, 9 to 117). Alternatively, 13 patients (41%) experienced relapse after initial complete response, with a median of 22 months (range, 8 to 45) and were considered as relapsing patients together with 5 patients (15%) refractory to treatment (RR, n=18). The median follow-up was 38 months (range, 8 to 117). The median disease-free period was 23 months (range, 0 to 117). Patients had a poor prognosis with 5-year overall survival rate at 38%, 95% CI (18% to 58%). Half of patients (n=16) died during the follow-up period, 9 (56%) related to lymphoma and 7 (44%) unrelated to the disease.

Lymphopanel sequencing at diagnosis:

Lymphopanel analysis was performed by next-generation sequencing (NGS) of the 32 PCLBCL-LT primary samples. For 8 patients, sequencing data of both tumoral and matched normal DNA at diagnosis were already available (Mareschal et al., 2017). The median overall sequencing depth was 1614x (range, 813 to 2716). When frozen biopsy was available (21/32 samples), comparison of NGS data from FFPE DNA and frozen DNA at diagnosis showed an increase in C to T transitions in FFPE samples related to formalin-induced changes (Spencer et al., 2013). Such artefactual variants had a low variant allele frequency (VAF) fewer than 5%.

The median of mutation per patient was 6 (range, 0 to 16). The median VAF was 34% with a range of 6 to 85% and discrepancy of VAF in the same tumor sample also suggested the combination of clonal and subclonal mutations (**Supplementary Table S2 online**). As expected, we observed a high prevalence of mutations in *PIM1* (69%), *MYD88* (69%), *IRF4* (16%) leading to NF-κB pathway activation and in *CD79B* (56%) leading to BCR pathway activation (**Figure 1**). Most of *MYD88* mutations corresponded to the mutational hotspot p.L265P except for two patients with p.V217F and p.S219C mutations, previously reported in

nodal DLBCL (Dubois et al., 2016; Ngo et al., 2011). *PIM1*, *IRF4*, *GNA13, CD58*, *ARID1A* and *MYC* frequently displayed more than one somatic mutation per patient and we investigated if aberrant somatic hypermutation (aSHM) involved the following genes: *IRF4, XPO1, MYC, PIM1, BCL2, CARD11, CD58, MYD88, CD79B, ARID1A, GNA13* by searching SNV at AID motif (DGYW/WRCH) (Rogozin and Pavlov, 2006). Indeed, 33% to 100% of observed SNV appeared as fingerprint of AID activity for *IRF4, XPO1, MYC, PIM1, BCL2, CARD11* and *CD58* genes but not for *MYD88, CD79B, GNA13* and *ARID1A* **(Supplementary Figure S1 online)**.

CDKN2A deletion was the most frequent copy number variation (CNV) observed (21/32 patients) with 11 homozygous and 10 heterozygous deletions **(Figure 1)**. *CDKN2B* was also deleted in 9 cases (28%) with 5 heterozygous and 4 homozygous deletions. Other deletions involved *PRDM1* (28%), *TNFAIP3* (19%) and *TP53* (13%). Interestingly, one heterozygous deletion of either *PRDM1* or *TNFAIP3* was associated with a stop gain mutation on the second copy leading to complete inactivation of the gene in each patient (n=2).

Copy gains detected for *BCL2* (19%) and *MYC* (6%) were confirmed by interphase fluorescence *in situ* hybridization (FISH). CNV analysis also indicated the presence of an amplification of *MYC* (>25 copies) and *BCL2* (>6 copies), in a relapsing/refractory patient (RR16).

Relapsing/refractory patients to R-PCT displayed mutations targeting BCR pathway:

Mutations of *CD79A/B* encoding for BCR subunits, were frequent (n=20, 62%). Two RR patients had a splice mutation in CD79A ITAM region consisting in a deletion across the intron 4/exon 5 that removes a part of ITAM domain, including the first tyrosine. *CD79B* mutations detected in 18 patients exclusively involved the ITAM domain and targeted the first tyrosine residue (Y196) except in one patient with E197D mutation **(Supplementary Figure**

S2 online). *CARD11* mutations on the coiled-coil domain detected in two patients were mutually exclusive with those of *CD79A/B* **(Supplementary Figure S2 online)**.

At presentation, the three patients at T3 stage displayed a mutation involving the BCR pathway **(Table 1)**.

A reduced progression free survival (PFS) was observed in patients with a *CD79B* mutation (median 18 months versus 45 months in wild-type group, Log-rank, *P*=0.05) **(Figure 2A).** A mutation among *CD79A* or *CD79B* genes was also associated with a reduced PFS (median 22 months versus not reached in the wild-type group, Log-rank, *P*=0.02) **(Figure 2B)** and a lower proportion of response to R-PCT (75% vs 25%, *P*=0.01) **(Table 1)**. Altogether, patients with mutation of either *CD79A/B* or *CARD11* encoding for members of the BCR signaling pathway displayed a reduced PFS and specific survival (SS) (median 18 months, Log-rank, *P*=0.002 and median 51 months, Log-rank, *P*=0.03 respectively, median durations were not reached in the wild-type group) **(Figure 3)** but not a reduced overall survival (OS) (median 48 months versus not reached in the wild-type group Log-rank, *P*=0.21) **(Supplementary Figure S3 online)**. Alternatively, a wild-type status of these genes was associated with R-PCT response (90% vs 23%) (*P*=0.0006) **(Table 1)**. There was no statistically significant difference of baseline treatment regimen (R-PCT with or without anthracycline) according to therapeutic response and BCR mutational status (*P*=1.00 and *P*=0.44 respectively) (Table 1). The *MYD88* mutated status had no adverse impact on PFS or OS but might be associated with a better SS (p=0.05) (**Supplementary Figure S4 online**). In the different MYD88wt/MYD88mt/BCRwt/BCRmt status combinations, a negative impact on SS, OS and PFS was only observed for patients with BCRmt status whatever MYD88 status, although the small size of each subgroup did not permit do reach statistical significance.

Clonal selection and heterogeneity between primary and secondary samples:

In 14 RR PCLBCL-LT, the analysis was conducted at diagnosis and at relapse or progression. Corrected VAF of each mutation was adapted to the estimated fraction of tumoral cells (**Figure 4**).

In 3 patients (RR5, RR6 and RR15), no major variation in corrected VAF was observed between the biopsy pairs. VAF enrichment of primary mutations affecting *CD79B* (patients RR11, RR17 and RR18), *CARD11* (patient RR2) and *MYD88* (patients RR11 and RR17) was observed at relapse or progression supporting a pivotal role in disease oncogenesis. Similarly, several mutants of *SOCS1, MYC* and *MYD88* had a very low VAF or even wild-type status at diagnosis and were enriched at relapse or progression. For example, an increase (from 1% to 58%) of the VAF of a *SOCS1* mutation was observed at relapse in patient RR18. A similar increase from <1% to 48% of $MYD88^{P258L}$ mutant VAF was observed in patient RR9 who also gained at progression two *MYC* mutations at a VAF around 50%.

Alternatively, a loss of mutation at relapse was observed for the following genes: *B2M* (RR3), *IRF4* (RR7, RR9), *CREBBP* (RR10), *CD79B* (RR10), *CARD11* (RR13) and *MEF2B* (RR12) **(Figure 4)**. To decipher differences between diagnosis and relapse in patient RR13, DNA from 3 tumor-rich macrodissected areas of the primary biopsy and from 2 areas of the relapse biopsy was subjected to re-sequencing. The *CARD11* mutation was detected at a VAF under 1% and equal to 9% in two areas of the primary biopsy while it was absent in the third area of the primary biopsy as opposed to 10% in global tissue. Other mutations of this case were homogeneously detected **(Table 2)**. No *CARD11* mutation was detected at relapse. Our data support both spatial intra-individual heterogeneity and temporal selection of subclones under treatment.

Finally, many patients displayed losses and gained mutations in the *PIM1* gene suggesting the presence of subclones carrying different *PIM1* mutations (patients RR3, RR9, RR10 and RR18). The bioinformatic analysis also revealed that somatic hypermutation load was higher

at relapse than at diagnosis supporting an ongoing aberrant hypermutation process **(Supplementary Figure S5 online)**.

DISCUSSION:

So far, the mutational profile of PCLBCL-LT had not been evaluated according to outcome or therapeutic response (Mareschal et al., 2017; Zhou et al., 2018). The comparison between 14 patients with durable response to R-PCT and 18 patients with relapsing or refractory disease highlights the central role of mutations involving the BCR pathway enriched in patients with poor PFS and therapeutic resistance.

In the relapsing/refractory group, a single case (RR16) harbored an amplification of *MYC* and *BCL2* polysomy which may account for therapeutic resistance (Mareschal et al., 2017). Indeed, MYC and BCL2 co-expression called dual expressor phenotype identifies a subgroup of patients with PCLBCL-LT and adverse prognosis (Menguy et al., 2018a).

Unlike our previous report on 58 PCLBCL-LT cases (Pham-Ledard et al., 2014), no adverse prognostic value of the $MYD88^{L265P}$ mutation was found. Here, only patients treated by R-PCT were included and diagnostic criteria for PCLBCL-LT have been improved (Menguy et al., 2016, 2018a, 2019).

Alternatively, mutations involving the BCR pathway were found associated with disease aggressiveness. The BCR is composed of a membrane-anchored surface immunoglobulin with an antigen-binding site on the variable regions and heterodimeric subunits, CD79A and B, which transduces signals to the cell (Davis et al., 2010). Antigenic stimulation of BCR signaling engages CARD11 a scaffolding protein that is part of the CBM multiprotein complex (CARD11/BCL10/MALT1) initiating NF-κB signaling (Davis et al., 2010; Ngo et al., 2006). Cell survival of ABC DLBCL depends on “chronic active” BCR signaling (Davis et al., 2010). *CD79A/B* mutations (20% in ABC DLBCL) increase “chronic BCR signaling”

by enhancing surface BCR expression and attenuating LYN kinase, a negative regulator of BCR activation (Davis et al., 2010; Heizmann et al., 2010). Chronic BCR is also dependent of *CARD11* mutations in 10% of ABC DLBCL leading to activation of the anti-apoptotic NF-κB pathway (Lenz et al., 2008; Davis et al., 2010). Addiction of ABC tumor cells to BTK signaling was shown by genetic interference for *CD79A/B*, *CARD11* or $MYD88^{L265P}$ mutations (Davis et al., 2010; Ngo et al., 2006). Distinct subgroups of DLBCL have been defined by the cell of origin or differentiation stage from which they develop that also matches with initiating or acquired genetic lesions (Schmitz et al., 2018). Among them, the MCD genetic subtype correspond to cases with both $MYD88^{L265P}$ and *CD79B* mutations predominantly observed in the ABC subgroup of DLBCL with frequent extranodal secondary involvement or primary onset such as PCNSL (Schmitz et al., 2018). This MCD genetic subtype was associated with shorter PFS and OS than the other subgroups of DLBCL but PCLBCL-LT was not evaluated (Schmitz et al., 2018). The MCD genotype present in 15 out of our 32 PCLBCL-LT cases (47%) was observed both in the CR (n=5, 36%) and the RR (n=10, 56%) subgroups without prognostic impact. In fact, therapeutic resistance was associated with mutations targeting one of the BCR signaling genes (*CD79A/B* or *CARD11).*

Ibrutinib is a selective inhibitor of BTK that kills ABC DLBCL lines by reducing NF-κB pathway activity (Davis et al., 2010; Yang et al., 2012). Interestingly, frequent responses were observed in ABC DLBCL with combined *CD79A/B* and $MYD88^{L265P}$ mutations (Wilson et al., 2015). Partial response to ibrutinib in PLBCL-LT has also been reported in some relapsing/refractory PCLBCL-LT (Fox et al., 2018; Gupta et al., 2015). In 18 PCNSL, a phase Ib study of ibrutinib monotherapy followed by ibrutinib plus chemotherapy provided a good response rate in patients with *CD79B* and/or *MYD88* mutations but not those with *CARD11* mutations, as also observed in nodal DLBCL (Lionakis et al., 2017; Wilson et al., 2015).

Moreover, the assessment of tumors pairs at diagnosis and at relapse or progression in 14 patients showed subclonal variations. One half of patients retained the same mutational profile at relapse while the other half harboured genetic changes in the relapse besides common genetic driver mutations at high VAF of *MYD88* and *CD79B* (Mareschal et al., 2017). The study of primer pairs also confirms sustained AID activity preferentially targeting the *PIM1* gene (Mareschal et al., 2017). The ongoing emergence of *PIM1* mutations in PCLBL-LT could also contribute to ibrutinib resistance observed in *PIM1* mutated ABC subtype of DLBCL (Kuo et al., 2016).

This study indicates that the mutational profile of PCLBCL-LT could help to predict therapeutic response to first-line R-PCT with resistance in patients bearing mutations of the BCR pathway. In such patients, ibrutinib could be proposed either in association with R-PCT or as a second-line therapy in patients without *CARD11* or *PIM1* mutations. Alternative therapies using lenalidomide, a modulator of NF-κB and IFNβ signaling, demonstrated effectiveness in some patients with relapsing/refractory PCLBCL-LT (Beylot-Barry et al., 2018). The toxicity and adverse effects of either ibrutinib or lenalidomide in this elderly population underscore the need of further deciphering mechanisms of therapeutic response.

MATERIALS AND METHODS:

Inclusion criteria and number of subjects:

All PCLBCL-LT patients were treated by R-PCT as first line therapy and included between 01/01/2004 and 01/07/2017 in the database of the French Study group on cutaneous lymphomas (GFLEC). All patients have been included in previous observational retrospective studies with informed consent and/or included in a phase II clinical trial (NCT01556035, REVLEG) that evaluate Lenalidomide in second line after R-PCT (Beylot-Barry et al., 2018). Clinical data were available or updated.

At diagnosis formalin-fixed, paraffin-embedded (FFPE) skin biopsy was available in 32 patients with 21-matched tumor frozen material. For 14 out of the 18 relapse or refractory patients after R-PCT therapy, we also had a FFPE skin biopsy at relapse before the second line treatment. According to the French public Health and Bioethical Law, no ethics committee approval was needed for this observational study on already collected data and biological material (Article L1121-1 and Article R1121-3). Moreover, informed written consent was given by patients for use of their data and biological material for research purposes.

Response to treatment:

Patients were followed during six R-PCT perfusions with an intermediate evaluation after three cures. Then, there was at least a half-yearly follow-up assessing potential relapse (Cheson et al., 2014). Patients were classified as follows:

1- Complete response (CR) was defined by a complete durable response lasting at least 6 months: disappearance of all lesions by clinical and radiological evaluation and without relapse during the study.

2- Relapsing/refractory (RR) patients were either:

- Refractory patients with no CR under R-PCT (Partial response*, stability** or progression***),

- Relapsing patients with apparition of new lesions after an initial complete response.

Immunohistochemistry:

FFPE slides were subjected to automated immunolabeling (Bond Max, Leica, France) with the following antibodies; BCL2 (clone 124, Dako), MUM1 (clone MUM1p, Dako), CD10 (clone 56C6, Leica), BCL6 (clone PGB6P, Dako), CD21 (clone 2G9, Leica), Ki67 (clone

MM1, Leica), CD20 (clone L26, Dako). The positivity cut-offs for BCL2, MUM1, or CD10 were respectively ⩾50%, ⩾30%, and ⩾30% of cells (Menguy et al., 2019).

Targeting next-generation sequencing using a lymphopanel comprising 36 genes:

DNA was extracted from FFPE and frozen tissues. Lymphopanel was designed to identify alterations within 36 genes important for lymphomagenesis, based on literature data and WES of relapsed/refractory DLBCL sequencing. A previous version has been used to characterize a PCLBCL-LT cohort (Dubois et al., 2016; Mareschal et al., 2017). The Ampliseq panel (ThermoFisher Scientific, Life Technologies, Les Ullis France) covers 75.08 kbases and was sequenced on IonS5. Data analysis was performed using Torrent Suite™ version 5.6 software (ThermoFisher Scientific). Reads were mapped to the human hg19 reference genome. The Variant Caller detected SNV with VAF ≥2% and INDEL with VAF ≥5%. VCF files were annotated by ANNOVAR (Wang et al., 2010). BAM sequence were also checked using Alamut Software (Interactive Biosoftware, Rouen, France). CNV were screened using the ONCOCNV algorithm (Boeva et al., 2014) compared to 7 control DNA patients.

Interphase fluorescence *in situ* hybridization (FISH):

To confirm copy number variation detected by sequencing analysis, hybridization was performed to evaluate *BCL2*, *MYC* and *CDKN2A* copy number (Menguy et al., 2018b; Pham-Ledard et al., 2013). Slides were analyzed by two independent observers. Gain was defined by presence of more than 4 copies, amplification by more than 6 copies and a ratio to a control locus above 2 and losses by less than 2 copies.

Statistical analysis:

Comparison of clinical characteristics and response according to mutational status was performed using Fisher's exact test. Patients without event of interest were censored at their last study visit, with administrative end of follow-up in July 2018. Disease-specific survival was calculated from diagnosis to disease-related death, and considering patients whose death was unrelated to lymphoma as censored. Overall survival duration was calculated from diagnosis to death from any cause and progression-free survival from the diagnosis to recurrence or disease-related death, whichever comes first. Kaplan-Meier survival curves were displayed. Statistical analyses were performed using Medcalc software (Ostend, Belgique) with a bilateral significance threshold of 0.05.

DATA AVAILABILITY POLICY:

Sequencing data were deposited in SRA database under NCBI accession PRJNA532525.

CONFLICT OF INTEREST:

- Marie Beylot-Barry: Research funding: Celgene; advisory board member: Roche, Takeda, Principal Investigator: Celgene, Galderma, Kyowa Hakko, Millenium, Roche, Biocryst, ArgenX.
- Fabrice Jardin: Personnal fees and travel accommodations: Janssen, Celgene, Roche, Amgen, Gilead. Research funding: Roche, Celgene.

ACKNOWLEDGMENTS:

The project was supported by the Société Française de Dermatologie with funding to Océane Ducharme and Ligue contre le Cancer, Comité de Dordogne. We thank Elodie Laharanne for FISH experiments, Martina Prochazkova-Carlotti for statistical analysis and the cancer biobank of University Hospital of Bordeaux. The following members of the French Study

Group of Cutaneous Lymphoma (GFELC) provided clinical data or pathological material: Laurent Mortier and Romain Dubois (CHU Lille, Lille France), Stephane Dalle and Brigitte Balme (CHU Lyon, Lyon, France), Anne Benedicte Duval Deste and Philippe Courville (CHU Rouen, Rouen, France), Eve Maubec and Lydia Deschamps (CHU Bichat, Paris, France) and Saskia Oro and Nicolas Ortonne (CHU Henri-Mondor, Créteil, France).

AUTHOR COTRIBUTIONS:

Conceptualization: OD, MBB, APL, FJ, JPM and AG; Data curation: PJV and TB; Formal Analysis: OD, AG and EF performed statistical analysis; Funding Acquisition: OD and AG Investigation: MBB, APL and OD collected clinical data. JPM and BV performed histological analysis. NF and EB performed targeted sequencing experiments. OD and AG performed fluorescent in situ hybridization analysis. Writing - Original Draft Preparation: OD, MBB, JPM and AG; Writing - Review and Editing: OD, MBB, JPM and AG.

REFERENCES:

Alizadeh AA, Eisen MB, Davis RE, Ma C, Lossos IS, Rosenwald A, et al. Distinct types of diffuse large B-cell lymphoma identified by gene expression profiling. Nature 2000;403:503–11.

Bachy E, Salles G. Are we nearing an era of chemotherapy-free management of indolent lymphoma? Clin Cancer Res Off J Am Assoc Cancer Res 2014;20:5226–39.

Beylot-Barry M, Mermin D, Maillard A, Bouabdallah R, Bonnet N, Duval-Modeste A-B, et al. A Single-Arm Phase II Trial of Lenalidomide in Relapsing or Refractory Primary Cutaneous Large B-Cell Lymphoma, Leg Type. J Invest Dermatol 2018.

Boeva V, Popova T, Lienard M, Toffoli S, Kamal M, Le Tourneau C, et al. Multi-factor data normalization enables the detection of copy number aberrations in amplicon sequencing data. Bioinformatics 2014;30:3443–50.

Chao MP. Treatment challenges in the management of relapsed or refractory non-Hodgkin's lymphoma - novel and emerging therapies. Cancer Manag Res 2013;5:251–69.

Cheson BD, Fisher RI, Barrington SF, Cavalli F, Schwartz LH, Zucca E, et al. Recommendations for initial evaluation, staging, and response assessment of Hodgkin and non-Hodgkin lymphoma: the Lugano classification. J Clin Oncol Off J Am Soc Clin Oncol 2014;32:3059–68.

Davis RE, Ngo VN, Lenz G, Tolar P, Young RM, Romesser PB, et al. Chronic active B-cell-receptor signalling in diffuse large B-cell lymphoma. Nature 2010;463:88–92.

Dubois S, Viailly P-J, Mareschal S, Bohers E, Bertrand P, Ruminy P, et al. Next-Generation Sequencing in Diffuse Large B-Cell Lymphoma Highlights Molecular Divergence and Therapeutic Opportunities: a LYSA Study. Clin Cancer Res Off J Am Assoc Cancer Res 2016;22:2919–28.

Fox LC, Yannakou CK, Ryland G, Lade S, Dickinson M, Campbell BA, et al. Molecular Mechanisms of Disease Progression in Primary Cutaneous Diffuse Large B-Cell Lymphoma, Leg Type during Ibrutinib Therapy. Int J Mol Sci 2018;19.

Grange F, Beylot-Barry M, Courville P, Maubec E, Bagot M, Vergier B, et al. Primary cutaneous diffuse large B-cell lymphoma, leg type: clinicopathologic features and prognostic analysis in 60 cases. Arch Dermatol 2007;143:1144–50.

Grange F, Joly P, Barbe C, Bagot M, Dalle S, Ingen-Housz-Oro S, et al. Improvement of survival in patients with primary cutaneous diffuse large B-cell lymphoma, leg type, in France. JAMA Dermatol 2014;150:535–41.

Gupta E, Accurso J, Sluzevich J, Menke DM, Tun HW. Excellent Outcome of Immunomodulation or Bruton's Tyrosine Kinase Inhibition in Highly Refractory Primary Cutaneous Diffuse Large B-Cell Lymphoma, Leg Type. Rare Tumors 2015;7:6067.

Heizmann B, Reth M, Infantino S. Syk is a dual-specificity kinase that self-regulates the signal output from the B-cell antigen receptor. Proc Natl Acad Sci U S A 2010;107:18563–8.

Hoefnagel JJ. Distinct types of primary cutaneous large B-cell lymphoma identified by gene expression profiling. Blood 2005;105:3671–8.

Koens L, Zoutman WH, Ngarmlertsirichai P, Przybylski GK, Grabarczyk P, Vermeer MH, et al. Nuclear Factor-κB Pathway–Activating Gene Aberrancies in Primary Cutaneous Large B-Cell Lymphoma, Leg Type. J Invest Dermatol 2014;134:290–2.

Kuo H-P, Ezell SA, Hsieh S, Schweighofer KJ, Cheung LW, Wu S, et al. The role of PIM1 in the ibrutinib-resistant ABC subtype of diffuse large B-cell lymphoma. Am J Cancer Res 2016;6:2489–501.

Lenz G, Davis RE, Ngo VN, Lam L, George TC, Wright GW, et al. Oncogenic CARD11 mutations in human diffuse large B cell lymphoma. Science 2008;319:1676–9.

Lionakis MS, Dunleavy K, Roschewski M, Widemann BC, Butman JA, Schmitz R, et al. Inhibition of B Cell Receptor Signaling by Ibrutinib in Primary CNS Lymphoma. Cancer Cell 2017;31:833–843.e5.

Mareschal S, Pham-Ledard A, Viailly PJ, Dubois S, Bertrand P, Maingonnat C, et al. Identification of Somatic Mutations in Primary Cutaneous Diffuse Large B-Cell Lymphoma, Leg Type by Massive Parallel Sequencing. J Invest Dermatol 2017;137:1984–94.

Menguy S, Beylot-Barry M, Marie P, Pham Ledard A, Frison E, Comoz F, et al. Primary Cutaneous Large B-Cell Lymphomas: relevance of the 2017 WHO Classification. Histopathology 2019.

Menguy S, Frison E, Prochazkova-Carlotti M, Dalle S, Dereure O, Boulinguez S, et al. Double-hit or dual expression of MYC and BCL2 in primary cutaneous large B-cell lymphomas. Mod Pathol Off J U S Can Acad Pathol Inc 2018a.

Menguy S, Gros A, Pham-Ledard A, Battistella M, Ortonne N, Comoz F, et al. MYD88 Somatic Mutation Is a Diagnostic Criterion in Primary Cutaneous Large B-Cell Lymphoma. J Invest Dermatol 2016;136:1741–4.

Menguy S, Prochazkova-Carlotti M, Beylot-Barry M, Saltel F, Vergier B, Merlio J-P, et al. PD-L1 and PD-L2 Are Differentially Expressed by Macrophages or Tumor Cells in Primary Cutaneous Diffuse Large B-Cell Lymphoma, Leg Type. Am J Surg Pathol 2018b;42:326–34.

Ngo VN, Davis RE, Lamy L, Yu X, Zhao H, Lenz G, et al. A loss-of-function RNA interference screen for molecular targets in cancer. Nature 2006;441:106–10.

Ngo VN, Young RM, Schmitz R, Jhavar S, Xiao W, Lim K-H, et al. Oncogenically active MYD88 mutations in human lymphoma. Nature 2011;470:115–9.

Pham-Ledard A, Beylot-Barry M, Barbe C, Leduc M, Petrella T, Vergier B, et al. High frequency and clinical prognostic value of MYD88 L265P mutation in primary cutaneous diffuse large B-cell lymphoma, leg-type. JAMA Dermatol 2014;150:1173–9.

Pham-Ledard A, Cappellen D, Martinez F, Vergier B, Beylot-Barry M, Merlio J-P. MYD88 somatic mutation is a genetic feature of primary cutaneous diffuse large B-cell lymphoma, leg type. J Invest Dermatol 2012;132:2118–20.

Pham-Ledard A, Prochazkova-Carlotti M, Andrique L, Cappellen D, Vergier B, Martinez F, et al. Multiple genetic alterations in primary cutaneous large B-cell lymphoma, leg type support a common lymphomagenesis with activated B-cell-like diffuse large B-cell lymphoma. Mod Pathol 2013.

Rogozin IB, Pavlov YI. The cytidine deaminase AID exhibits similar functional properties in yeast and mammals. Mol Immunol 2006;43:1481–4. doi:10.1016/j.molimm.2005.09.002.
Schmitz R, Wright GW, Huang DW, Johnson CA, Phelan JD, Wang JQ, et al. Genetics and Pathogenesis of Diffuse Large B-Cell Lymphoma. N Engl J Med 2018;378:1396–407.

Schmitz R, Wright GW, Huang DW, Johnson CA, Phelan JD, Wang JQ, et al.. Genetics and Pathogenesis of Diffuse Large B-Cell Lymphoma. N Engl J Med. 2018 Apr 12; 378(15):1396-1407.

Senff NJ, Noordijk EM, Kim YH, Bagot M, Berti E, Cerroni L, et al. European Organization for Research and Treatment of Cancer and International Society for Cutaneous Lymphoma consensus recommendations for the management of cutaneous B-cell lymphomas. Blood 2008;112:1600–9.

Spencer DH, Sehn JK, Abel HJ, Watson MA, Pfeifer JD, Duncavage EJ. Comparison of clinical targeted next-generation sequence data from formalin-fixed and fresh-frozen tissue specimens. J Mol Diagn JMD 2013;15:623–33.

Swerdlow SH, Campo E, Pileri SA, Harris NL, Stein H, Siebert R, et al. The 2016 revision of the World Health Organization classification of lymphoid neoplasms. Blood 2016;127:2375–90.

Wang K, Li M, Hakonarson H. ANNOVAR: functional annotation of genetic variants from high-throughput sequencing data. Nucleic Acids Res 2010;38:e164.

Willemze R, Cerroni L, Kempf W, Berti E, Facchetti F, Swerdlow SH, et al. The 2018 update of the WHO-EORTC classification for primary cutaneous lymphomas. Blood 2019.

Willemze R, Jaffe ES, Burg G, Cerroni L, Berti E, Swerdlow SH, et al. WHO-EORTC classification for cutaneous lymphomas. Blood 2005;105:3768–85.

Wilson WH, Young RM, Schmitz R, Yang Y, Pittaluga S, Wright G, et al. Targeting B cell receptor signaling with ibrutinib in diffuse large B cell lymphoma. Nat Med 2015;21:922–6.

Yang Y, Shaffer AL, Emre NCT, Ceribelli M, Zhang M, Wright G, et al. Exploiting synthetic lethality for the therapy of ABC diffuse large B cell lymphoma. Cancer Cell 2012;21:723–37.

Zhou XA, Louissaint A, Wenzel A, Yang J, Martinez-Escala ME, Moy AP, et al. Genomic Analyses Identify Recurrent Alterations in Immune Evasion Genes in Diffuse Large B-Cell Lymphoma, Leg Type. J Invest Dermatol 2018;138:2365–76.

Tables :

Table 1: Main Findings at diagnosis and follow-up data according to (i) *CD79A/B* (ii) *CD79A/B* or *CARD11* mutation (BCR mutation).

		CD79A/B			BCR mutation		
Characteristics	**Total**	**WT**	**Mutation**	**P Value[a]**	**WT**	**Mutation**	**P Value[b]**
Patients, n (%)	32 (100)	12 (38)	20 (62)		10 (31)	22 (69)	
Age at diagnosis, median (range) (y)	81 (61-97)	82 (61-97)	81 (62-94)		79,5 (61-97)	82,5 (62-94)	
Female sex, n (%)	19 (59)	9 (75)	10 (50)	P=0.27	8 (80)	11 (50)	P=0.14
Localization, n (%)							
Lower limb	27 (84)	10 (83)	17 (85)	P= 0.99	8 (80)	19 (86)	P=0.64
Other site	5 (16)	2 (17)	3 (15)		2 (20)	3 (14)	
LDH							
Normal	23 (72)	10 (83)	13 (65)	P=0.42	9 (90)	14 (64)	P=0.21
High	9 (28)	2 (16)	7 (35)		1 (10)	8 (36)	
T stage, n (%)							
T1	9 (28)	5 (42)	4 (20)		5 (50)	4 (18)	
T2	20 (63)	7 (58)	13 (65)	P=0.21	5 (50)	15 (68)	P=0.12
T3	3 (9)	0 (0)	3 (15)		0 (0)	3 (14)	
Extracutaneous spreading, n (%)	9 (28)	2 (16)	7 (35)	P=0.70	1 (10)	8 (36)	P=0.27
Type of treatment regimens, n (%)							
R-PCT with anthracycline	22 (69)	9 (75)	13 (65)	P= 0,70	8 (80)	14 (64)	P= 0,44
R-PCT without anthracycline	10 (31)	3 (25)	7 (35)		2 (20)	8 (36)	
Outcome, n (%)							
Durable complete responders (CR)	14 (44)	9 (75)	5 (25)	**P=0.01**	9 (90)	5 (23)	**P=0.0006**
Refractory/Relapse (RR)	18 (56)	3 (25)	15 (75)		1 (10)	17 (77)	
* Relapse after CR	13 (41)	3 (25)	10 (50)	P=0.52	1 (10)	12 (54)	P=0.99
* Primary refractory	5 (15)	0 (0)	5 (25)		0 (0)	5 (23)	
Status at last follow-up, n (%)							
Alive disease free	12 (38)	6 (50)	6 (30)		6 (60)	6 (27)	
Alive with disease	4 (12)	1 (8)	3 (15)	P=0.72	1 (10)	3 (14)	P=0.12
Died of lymphoma	9 (28)	2 (17)	4 (20)		0 (0)	9 (41)	
Died unrelated	7 (22)	3 (25)	7 (35)		3 (30)	4 (18)	
Specific survival rates, %							
3-year survival	74	80	70	P=0.33[c]	100	63	**P=0.03**[c]
5-year survival	59	80	50		100	45	
Overall survival rates, %							
3-year survival	65	62	66	P=0.65[c]	76	59	P=0.21[c]
5-year survival	38	42	37		51	33	
Progression free survival, %							
3-year survival	42	82	24	**P=0.02**[c]	100	22	**P=0.002**[c]
5-year survival	32	61	18		75	16	

Abbreviation: WT, wild-type; CR, durable complete response; RR, Refractory/relapse; BCR: B-cell receptor

a Indicates the difference between patients exhibiting *CD79A/B* WT and those with a mutation in *CD79A/B* gene.

b Indicates the difference between patients exhibiting *CD79A/B* and *CARD11* WT and those with a mutation in *CD79A* or *CD79B* or in *CARD11* gene (BCR mutation).

c P values correspond to the comparison of survival curves.

Table 2: Intra-tumour heterogeneity in primary and relapse biopsy. Resequencing of several areas from the biopsy of the patient RR13 at the diagnosis and at the relapse.

First line corresponds to the mutations observed from the global tissue. The other lines correspond to the mutation from a distinct zone of the sample. In each column gene, the mutation and the VAF (%) are specified. At diagnosis, the *CARD11* mutation was detected in area 1 and 3 (low level) but absent in area 2. At relapse, no *CARD11* mutation was detected in any area.

	Zone of extraction	***ARID1A***	***NOTCH2***	***CCND3***	***TNFAIP3***	***CARD11***	***NOTCH1***
Primary	**Global Tissue**	c.6100G>A ; p.(Glu2034Lys) ; 40	c.7198C>T ; p.(Arg2400*) ; 71	c.778C>T; p.(Gln260*) ; 40	c.1880_1881del ; p.(Cys627Phefs*44) ; 65	c.1071C>G ; p.(Asp357Glu) ; 10	c.7538C>T ; p.(Ser2513Phe) ; 42
	Area 1	c.6100G>A ; p.(Glu2034Lys) ; 43	c.7198C>T ; p.(Arg2400*) ; 76	c.778C>T ; p.(Gln260*) ; 42	c.1880_1881del ; p.(Cys627Phefs*44) ; 63	c.1071C>G ; p.(Asp357Glu) ; **<1**	c.7538C>T ; p.(Ser2513Phe) ; 40
	Area 2	c.6100G>A ; p.(Glu2034Lys) ; 41	c.7198C>T ; p.(Arg2400*) ; 71	c.778C>T ; p.(Gln260*) ; 35	c.1880_1881del ; p.(Cys627Phefs*44) ; 71	**NA; 0 (0/2404 reads)**	c.7538C>T ; p.(Ser2513Phe) ; 38
	Area 3	c.6100G>A ; p.(Glu2034Lys) ; 32	c.7198C>T ; p.(Arg2400*) ; 66	c.778C>T ; p.(Gln260*) ; 30	c.1880_1881del ; p.(Cys627Phefs*44) ; 46	c.1071C>G ; p.(Asp357Glu) ; 9	c.7538C>T ; p.(Ser2513Phe) ; 34
Relapse	**Global Tissue**	c.6100G>A ; p.(Glu2034Lys) ; 35	c.7198C>T ; p.(Arg2400*) ; 55	c.778C>T; p. .(Gln260*) ; 30	c.1880_1881del ; p.(Cys627Phefs*44) ; 57	**NA; 0 (0/1786 reads)**	c.7538C>T ; p.(Ser2513Phe) ; 29
	Area 1	c.6100G>A ; p.(Glu2034Lys) ; 33	c.7198C>T ; p.(Arg2400*) ; 58	c.778C>T ; p.(Gln260*) ; 34	c.1880_1881del ; p.(Cys627Phefs*44) ; 43	**NA; 0 (0/2145 reads)**	c.7538C>T ; p.(Ser2513Phe) ; 35
	Area 2	c.6100G>A ; p.(Glu2034Lys) ; 44	c.7198C>T ; p.(Arg2400*) ; 72	c.778C>T ; p.(Gln260*) ; 46	c.1880_1881del ; p.(Cys627Phefs*44) ; 70	**NA; 0 (0/2567 reads)**	c.7538C>T ; p.(Ser2513Phe) ; 44

Figure legends:

Figure 1: Overview of the somatic mutations and CNV alterations detected by the lymphopanel.

(A) Each line represents one patient and each column represents one gene organized by symbols-coded (RRx= Relapsing/refractory patients and CRx= Durable complete responder patients):

❶ Missense. In the middle, the number of mutations observed is specified; ◆ Nonframeshift indel; × Stopgain comprising frameshift and nonsense mutations; ★ Splicing.

Shading indicates CNV observed for each gene: red shading indicates deletions, homozygous (dark) or heterozygous (light), blue shading indicates gains.

(B) Graph represents proportion of affected patients for each gene by mutations (black) or CNV (grey).

Figure 2: Kaplan-Meier survival curves for progression-free survival (PFS) in 32 patients with primary cutaneous diffuse large B-cell lymphoma leg type according to the mutational status of (A) *CD79B*, (B) *CD79A* or *B*.

(A) A *CD79B* mutation was detected in 18/32 patients with statistically significant difference for PFS (*P*=0.05).

(B) A *CD79A/B* mutation was present in 20/32 patients, with statistically significant difference for PFS (*P*=0.02).

Group 0 corresponds to wild type patients; Group 1 corresponds to mutated patients.

WT=Wild-type; MT= mutated.

Figure 3: Kaplan–Meier survival curves of 32 patients with primary cutaneous diffuse large B-cell lymphoma leg type according to the mutational status of the three genes implicated in the B-cell receptor (BCR) signaling pathway (*CARD11* and *CD79A/B*). (A) Progression-free survival (PFS), and (B) specific survival.

A BCR mutation was present in 22/32 patients, with statistically significant difference for PFS (*P*=0.002) and specific survival (*P*=0.03). Group 0 corresponds to wild-type patients; Group 1 corresponds to mutated patients.

WT = Wild-type; MT = mutated

Figure 4: Variations of corrected variant allelic frequencies of mutations in 14 tumors pairs from the same patient at diagnosis (P) and at relapse or progression (R).

The arrow indicates the time between the two biopsies in a same patient.

Supplementary Materials

Supplemental Table S1: Summary of immunophenotypical features of 32 PCLBCL-LT sequenced in this study.

Supplemental Table S2: Mutations observed at diagnosis in the lymphopanel for each patient.

Supplemental Figure S1: Aberrant somatic hypermutation analysis.

Supplemental Figure S2: Schematics of genes annotated with oncogenic mutations found in PCLBCL-LT at diagnosis.

Supplementary Figure S3: Overall survival for 32 patients with primary cutaneous diffuse large B-cell lymphoma leg type according to the mutational status of the three genes implicated in the B-cell receptor (BCR) signalling pathway (*CARD11* and *CD79A/B*).

Supplementary Figure S4: Specific survival for 32 patients with primary cutaneous diffuse large B-cell lymphoma leg type according to the mutational status of *MYD88*.

Supplemental Figure S5: Distribution of mutations for each gene between primary (P) and relapse or progression tumours (R) for the 14 RR patients analysed.

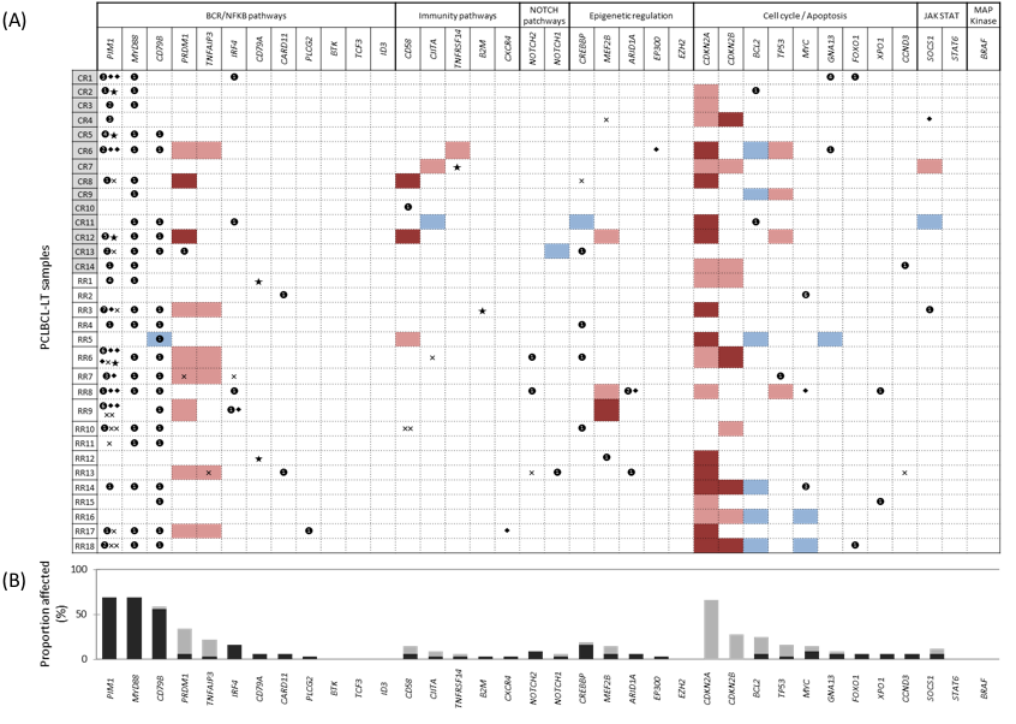
(A)
BCR/NFKB pathways
Immunity pathways
NOTCH patchways
Epigenetic regulation
Cell cycle / Apoptosis
JAK STAT
MAP Kinase
PIM1
MYD88
CD79B
PRDM1
TNFAIP3
IRF4
CD79A
CARD11
PLCG2
BTK
TCF3
ID3
CD58
CIITA
TNFRSF14
B2M
CXCR4
NOTCH2
NOTCH1
CREBBP
MEF2B
ARID1A
EP300
EZH2
CDKN2A
CDKN2B
BCL2
TP53
MYC
GNA13
FOXO1
XPO1
CCND3
SOCS1
STAT6
BRAF
PCLBCL-LT samples
CR1
CR2
CR3
CR4
CR5
CR6
CR7
CR8
CR9
CR10
CR11
CR12
CR13
CR14
RR1
RR2
RR3
RR4
RR5
RR6
RR7
RR8
RR9
RR10
RR11
RR12
RR13
RR14
RR15
RR16
RR17
RR18
(B)
Proportion affected (%)
100
50
0

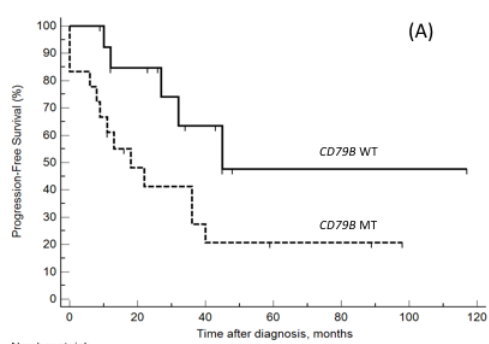
(A)
Progression-Free Survival (%)
100
90
80
70
60
50
40
30
20
10
0
CD79B WT
CD79B MT
0
20
40
60
80
100
120
Time after diagnosis, months
Number at risk
Group: 0
14 10 5 1 1 1 0
Group: 1
15 7 3 2 2 0 0

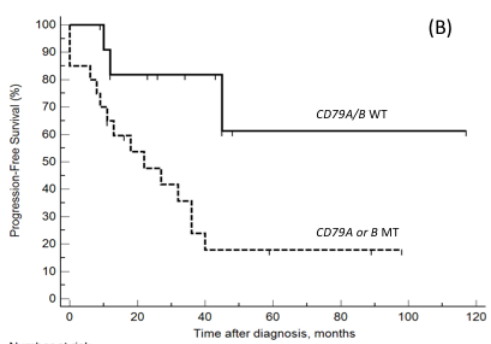
(B)
Progression-Free Survival (%)
100
90
80
70
60
50
40
30
20
10
0
CD79A/B WT
CD79A or B MT
0
20
40
60
80
100
120
Time after diagnosis, months
Number at risk
Group: 0
12 8 5 1 1 1 0
Group: 1
17 9 3 2 2 0 0

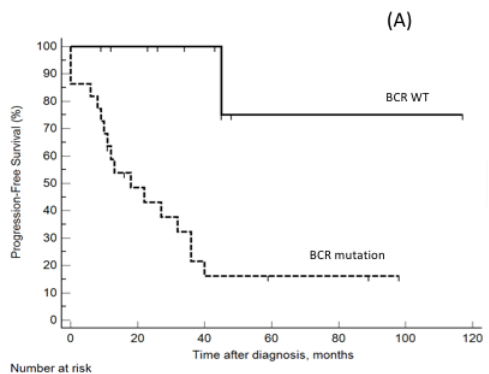
(A)
Progression-Free Survival (%)
100
90
80
70
60
50
40
30
20
10
0
BCR WT
BCR mutation
0
20
40
60
80
100
120
Time after diagnosis, months
Number at risk
Group: 0
10 8 5 1 1 1 0
Group: 1
19 9 3 2 2 0 0

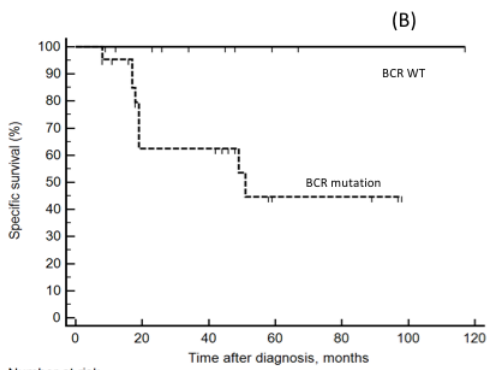
(B)
Specific survival (%)
100
90
80
70
60
50
40
30
20
10
0
BCR WT
BCR mutation
0
20
40
60
80
100
120
Time after diagnosis, months
Number at risk
Group: 0
10 8 5 2 1 1 0
Group: 1
22 11 11 3 3 0 0

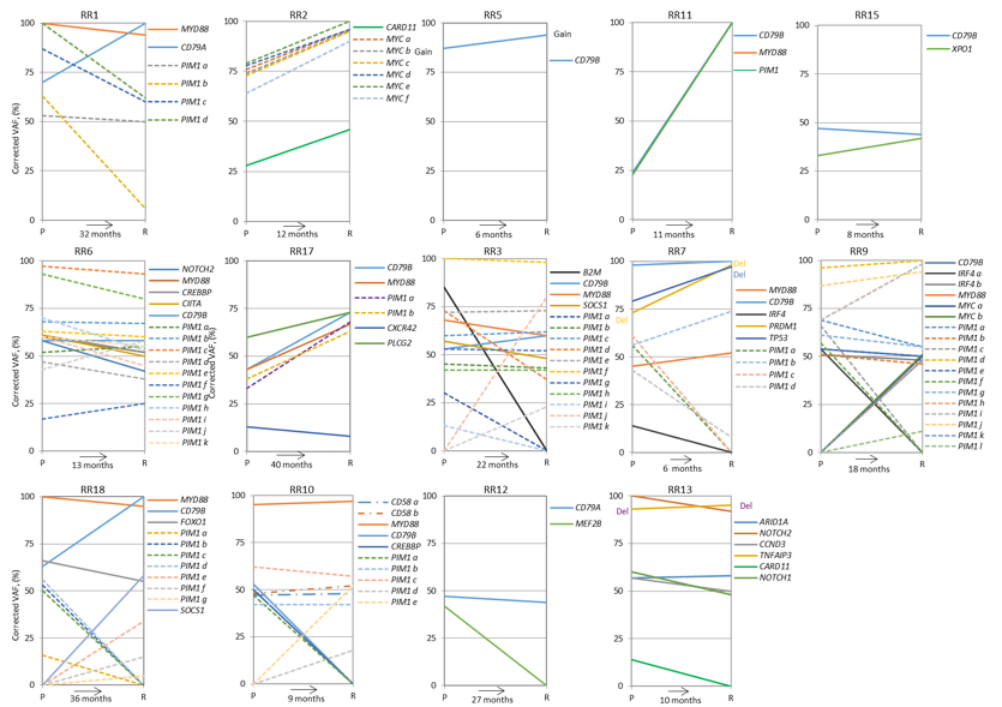
RR1
MYD88
CD79A
PIM1 a
PIM1 b
PIM1 c
PIM1 d
Corrected VAF, (%)
32 months
RR2
CARD11
MYC a
MYC b
MYC c
MYC d
MYC e
MYC f
12 months
RR5
Gain
Gain
CD79B
6 months
RR11
CD79B
MYD88
PIM1
11 months
RR15
CD79B
XPO1
8 months
RR6
NOTCH2
MYD88
CREBBP
CIITA
CD79B
PIM1 a
PIM1 b
PIM1 c
PIM1 d
PIM1 e
PIM1 f
PIM1 g
PIM1 h
PIM1 i
PIM1 j
PIM1 k
13 months
RR17
CD79B
MYD88
PIM1 a
PIM1 b
CXCR42
PLCG2
40 months
RR3
B2M
CD79B
MYD88
SOCS1
PIM1 a
PIM1 b
PIM1 c
PIM1 d
PIM1 e
PIM1 f
PIM1 g
PIM1 h
PIM1 i
PIM1 j
PIM1 k
22 months
RR7
Del
Del
Del
MYD88
CD79B
IRF4
PRDM1
TP53
PIM1 a
PIM1 b
PIM1 c
PIM1 d
6 months
RR9
CD79B
IRF4 a
IRF4 b
MYD88
MYC a
MYC b
PIM1 a
PIM1 b
PIM1 c
PIM1 d
PIM1 e
PIM1 f
PIM1 g
PIM1 h
PIM1 i
PIM1 j
PIM1 k
PIM1 l
18 months
RR18
MYD88
CD79B
FOXO1
PIM1 a
PIM1 b
PIM1 c
PIM1 d
PIM1 e
PIM1 f
PIM1 g
SOCS1
36 months
RR10
CD58 a
CD58 b
MYD88
CD79B
CREBBP
PIM1 a
PIM1 b
PIM1 c
PIM1 d
PIM1 e
9 months
RR12
CD79A
MEF2B
27 months
RR13
Del
Del
ARID1A
NOTCH2
CCND3
TNFAIP3
CARD11
NOTCH1
10 months
P
R